Sound speed requirements for optimal imaging of seismic oceanography data

Will F. J. Fortin[1] and W. Steven Holbrook[1]

Received 30 April 2009; revised 10 July 2009; accepted 16 July 2009; published 21 August 2009.

[1] Low-frequency acoustic imaging of internal oceanic structure (''seismic oceanography'') is providing unprecedented views of thermohaline finestructure with the potential to provide quantitative information on such processes as internal waves, eddy dynamics, and turbulent dissipation. Producing seismic images clear enough to confidently extract such information requires accurate sound-speed models. Because sound-speed modeling is time-intensive, and oceanic sound speed relatively simple compared to the solid earth, simplistic assumptions of ocean sound speeds have some appeal in seismic processing of ocean reflections. Here, we consider the effect on seismic images of four sound-speed models: (1) a uniform sound speed of 1500 m/s, (2) regional data from an archived database, (3) temperature profiles collected concurrently with the seismic data, and (4) standard user-selected profiles. Our results show the inadequacy of simple ''shortcut'' models (1 and 2) and indicate the necessity of rigorous, locally derived sound-speed models (3 and 4). **Citation:** Fortin, W. F. J., and W. S. Holbrook (2009), Sound speed requirements for optimal imaging of seismic oceanography data, *Geophys. Res. Lett.*, *36*, L00D01, doi:10.1029/2009GL038991.

1. Introduction

[2] Seismic oceanography (SO) is a recently developed approach for imaging thermohaline finestructure in the water column [*Holbrook et al.*, 2003]. Work to date includes high-resolution images of numerous oceanic features and processes, including internal wave strains and displacements [*Nandi et al.*, 2004; *Holbrook and Fer*, 2005; *Krahmann et al.*, 2008], currents [*Tsuji et al.*, 2005], fronts [*Holbrook et al.*, 2003; *Nakamura et al.*, 2006], eddies [*Biescas et al.*, 2008], boundary mixing (W. S. Holbrook et al., Estimating turbulent dissipation in the ocean from seismic reflection images, submitted to *Geophysical Research Letters*, 2009a; B. Biescas et al., Seismic imaging of staircases and boundary mixing in the deep ocean, submitted to *Geophysical Research Letters*, 2009), M_2 internal tides (W. S. Holbrook et al., Images of internal tides near the Norwegian continental slope, submitted to *Geophysical Research Letters*, 2009b), and lee waves (D. Eakin et al., Seismic images of lee waves on the Caribbean margin off Costa Rica, submitted to *Geophysical Research Letters*, 2009). Seismic reflection techniques are uniquely suited to imaging such features in their spatial context due to its dense lateral sampling (on the order of a few meters). As seismic oceanography matures, however, it is evolving from efforts to catalogue and explain images of various oceanographic phenomena, into a means of extracting quantitative information about temperature structure [*Páramo and Holbrook*, 2005; *Wood et al.*, 2008] and ocean mixing processes, such as turbulence dissipation [*Klymak and Moum*, 2007b; Holbrook et al., submitted manuscript, 2009a]. This places strict demands on the quality of processed seismic images, which must faithfully reproduce the strength, lateral continuity, and shape of thermohaline finestructure.

[3] The quality of a seismic image is heavily dependent on the processing steps that create it, especially the construction of a sound-speed model, which is necessary to correct for the geometry of reflecting rays. In typical seismic processing, construction of a sound-speed (or ''velocity'') model is a time-consuming step, due to the complexity and variability of seismic velocities in the solid earth. As seismologists turn their attention to imaging the water column, they may assume that the relative simplicity of sound speed in the ocean ($\sim$1500 m/s $\pm$ 2%) implies that careful construction of sound-speed profiles is less important than in typical seismic processing. Several shortcuts can be envisioned, such as a constant sound speed (e.g., 1500 m/s) or a regional sound-speed profile drawn from an archived database (e.g., Levitus); if permissible, these shortcuts would drastically reduce the time needed to process both newly acquired and the large quantity of legacy seismic data. However, these shortcuts may damage the final signal-to-noise ratio of the typically weak reflections recorded from water column sources. Additionally, an accurate sound-speed model in the water column will benefit imaging of sub-seafloor reflections, especially the thin upper sediments.

[4] Here, we investigate the sound-speed requirements for optimal processing of seismic oceanography data by examining the effects on a processed image of four different sound-speed models. Each model represents a different approach that might be taken to process SO data. In order of increasing complexity, the models are: (1) A constant speed of 1500 m/s. (2) A sound-speed profile derived from the nearest station in the Levitus database [*Levitus et al.*, 1994]. (3) A two-dimensional sound-speed model constructed from a dense array of XBTs (eXpendable BathyThermograph) deployed along the seismic line during seismic acquisition. (4) A user-selected (''handpicked'') sound-speed model created by the standard approach of flattening reflectors in common midpoint (CMP) gathers [*Yilmaz and Doherty*, 1987a, 1987b; *Sheriff and Geldart*, 1995]. For each model, we calculate the signal-to-noise ratio (S/N) of the resulting stacked, migrated seismic image and tally the number of reflections that can be tracked using an automated tracking algorithm.

[5] Acceptable results were provided by both the XBT-based and the handpicked sound-speed models, with the

[1]Department of Geology and Geophysics, University of Wyoming, Laramie, Wyoming, USA.

0094-8276/09/2009GL038991

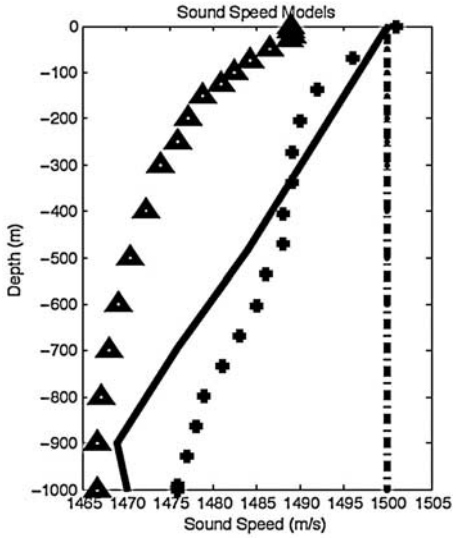

Figure 1. Sound speed plotted against depth for the 4 models: 1500 m/s (dot-dash), Levitus (triangles), representative XBT-derived (plus), and handpicked at same location as XBT (solid).

handpicked results being slightly superior. Images created using a constant sound speed or the archived sound-speed profile generated significantly lower signal-to-noise ratios. For optimal processing of seismic oceanography data, rigorous sound-speed models are a necessity, and shortcuts should be avoided.

2. Data Acquisition

[6] The seismic data analyzed here are from Line 11 in the Norwegian Sea and were acquired in September 2003 by the *R/V Maurice Ewing*. A six-gun acoustic source with a combined volume of 1340 cubic inches was fired every 37.5 meters. The reflected energy was recorded on a 6-kilometer streamer with hydrophone groups spaced every 12.5 meters at a sample rate of 2 milliseconds. Further discussion of line location and collection parameters from the survey are given by *Nandi et al.* [2004]. For this study we reprocessed a portion of Line 11 that comprised 13,001 common midpoint gathers (2,167 shots). This section was selected because it is a well-understood area and has dense XBT coverage consisting of 17 Sippican T-5 XBT drops collected at about 5-km intervals concurrently with the seismic data [*Nandi et al.*, 2004].

3. Methods

[7] After sorting into CMPs, the data were processed identically with the sole exception of the sound-speed model applied for normal move-out (NMO) and post-stack time migration. The four different models (Figure 1) were: (1) A constant speed of 1500 m/s. This could be considered the simplest possible assumption of sound speed in the ocean (the "maximum ignorance" model). (2) A sound-speed profile derived from the nearest station in the Levitus database [*Levitus et al.*, 1994]. This might represent an effort to describe the local oceanographic conditions in the absence of *in situ* measurements or time-consuming processing. (3) A two-dimensional sound-speed model constructed from seventeen XBTs (eXpendable BathyThermograph) deployed along the seismic line during seismic acquisition. This approach will become more common as joint PO/SO surveys are acquired; if viable, sound-speed models taken from coincident XBT data would save many person-hours of seismic data analysis for a relatively modest field expense. (4) A user-selected ("handpicked") sound-speed model created by flattening reflectors in common midpoint (CMP) gathers every 200 CMPs (1250 m). This is the standard approach in seismic data processing and by far the most time-consuming method for the user as reflections in the CMP (offset vs. time) domain must be visually inspected and matched to a hyperbolic move-out curve [*Yilmaz and Doherty*, 1987a, 1987b; *Sheriff and Geldart*, 1995]. The remainder of the processing flow consisted of muting stretched far-offset data, stacking the CMPs, filtering the data from 15–90 Hz, a seafloor mute, and finite-difference post-stack time migration using interval velocities derived from each of the four sound-speed models.

[8] The sound-speed model taken from the Levitus database was collected in September, 2004 at 65.5°N, 2.5°W. These data are very near (within ~50 km) the center of Line 11 and were acquired at the same time of year, one year after the seismic survey. The temperature profile was converted from temperature and depth to sound speed (c) using:

$$c = 1448.96 + 4.591T + 0.05304T^2 + 2.374 \times 10^{-4}T^3 + 1.34(S-35) + 1.63 \times 10^{-2}z + 1.675 \times 10^{-7}z^2 - 1.025 \times 10^{-2}T(S-35) - 7.139 \times 10^{-13}Tz^3 \quad (1)$$

[*Mackenzie*, 1981], where T is the temperature in degrees Celsius, z is the depth in meters, and S is the salinity in psu. We assumed a salinity of 35 psu, which is typical for the region [*Skagseth*, 2004; *Swift*, 1986] and a reasonable assumption due to the dominant role of temperature in acoustically imaging water column reflections [*Holbrook et al.*, 2003], but could be slightly improved with concurrently collected salinity measurements. NMO corrections were then applied using root-mean-square (RMS) sound speeds, which were calculated by dividing the sound-speed profiles into depth intervals and using:

$$c_{rms}^2 = \frac{\sum_{i=1}^{n} c_i^2 \Delta t_i}{\sum_{i=1}^{n} \Delta t_i}, \quad (2)$$

where c_i is the layer interval sound speed, and Δt_i is the one-way time it takes for sound to vertically traverse the layer.

[9] The XBT data were treated in a similar manner; sound speed was calculated using equation (1) and RMS sound speeds were calculated using equation (2). The complete, two-dimensional sound-speed model was created by assigning the sound-speed profile from each XBT drop to its corresponding CMP number in the processing flow.

[10] Reflections were tracked in the images using an automated approach based on contours of the cosine of the instantaneous phase angle of the data (Holbrook et al., submitted manuscript, 2009a). Reflections that could be

Table 1. Signal-to-Noise Ratio (S/N) and Number of Tracked Reflections for Each Sound-Speed Model Along the Entire Seismic Image in the Depth Range 300–600 m

Model	Signal-to-Noise	Number of Reflectors
1500 m/s	2.1	152
Levitus	2.8	717
XBTs	4.8	1725
Handpicked	4.8	2028

tracked laterally for at least 800 m (128 points) were tallied in Table 1.

4. Results and Conclusion

[11] The stacked images vary widely in quality depending on the sound-speed model applied during processing (Table 1). In general, data quality increases in the order of our numbered sound-speed models, with model 1 (1500 m/s) producing poor results and the handpicked sound speed producing the best results. The sound speed is used twice in the processing flow: first in the move-out for stacking and again in the migration. However, the sound-speed model has greater impact in the move-out and stacking. Reflected acoustic signal from water-column reflectors is very weak and so needs to be summed (stacked) with great accuracy. Migration affects the final image by better constraining the shape, location and detail of the reflection. While it is necessary to both stack and migrate with an optimal sound-speed model, we note that its primary effect is pre-migration. We discuss the results of each sound-speed model in detail below.

[12] Model 1 (a constant sound speed of 1500 m/s) produces only a few weak reflections (Figure 2a); the image has low signal-to-noise ratio (2.1, Table 1) and produces few reflections sufficiently well-defined to track laterally (n = 152). This result is not surprising, given that sound speeds on the profile are substantially lower than 1500 m/s (Figure 1). Model 1 works best in the upper ocean where the temperature is higher and the sound speed is closer to 1500 m/s (Figure 2a).

[13] Model 2 (the Levitus-derived sound speed) produces a moderately improved image with a signal-to-noise ratio of 2.8 and a greater number of reflectors (n = 717) than Model 1 (Figure 2b). Although the Levitus model represents a close match to location and season of the seismic data, ocean temperatures (and thus sound speed) in this area were substantially lower than those present during the seismic survey a year earlier (Figure 1). This results serves as an example of the risk of processing seismic data with sound speeds not derived directly from that data.

[14] Model 3 (the XBT-derived sound speed) produces an image with numerous (n = 1725), bright reflectors (Figure 2c) and a high signal-to-noise ratio (4.8). This image is sharp enough to detect detailed structures in the water column, such as a small eddy between 350–500 m depth around 47–55 km along line, and the internal waves given by *Nandi et al.* [2004] and described as M_2 internal tide beams by Holbrook et al. (submitted manuscript, 2009b) (Figure 3).

[15] Model 4 (handpicked sound speeds) produced an image (Figure 2d) with the greatest number of trackable reflections (n = 2028) and a signal-to-noise ratio equivalent to Model 3. The handpicked sound speeds are within ±5 m/s of the XBT sound speeds at all depths (Figure 1). Although the differences between the images produced by Models 3 and 4 are subtle, slight improvements in the clarity of the small eddy and M_2 beams are visible to the eye (Figure 3).

[16] The principal reason for the increased number of reflectors for Model 4 over that of Model 3 is improved lateral sampling of the sound-speed profiles: whereas XBTs were deployed at ~5 km lateral spacing, sound-speed profiles were handpicked at 1.25 km intervals. Model 4 thus more faithfully reproduces subtle lateral variability in ocean sound speed.

[17] These results have important consequences for future analyses of seismic oceanography data. Clearly, using simplified sound-speed models, whether it is a constant sound speed throughout the water column or an archived sound-speed profile, is perilous; some knowledge of the local conditions is required. We note that it is conceivable that in some cases, archived regional data will provide a good match to the conditions present during a given seismic survey, but relying on such good fortune is unwise. As approaches to extract more quantitative information about temperature and ocean mixing parameters become more common (Holbrook et al., submitted manuscript, 2009a; C. Papenberg et al., Ocean temperature and salinity inverted from seismic data, submitted to *Geophysical Research Letters*, 2009), accurate imaging becomes critical. Our results suggest that shortcuts, however tempting, are to be avoided in processing seismic oceanography data.

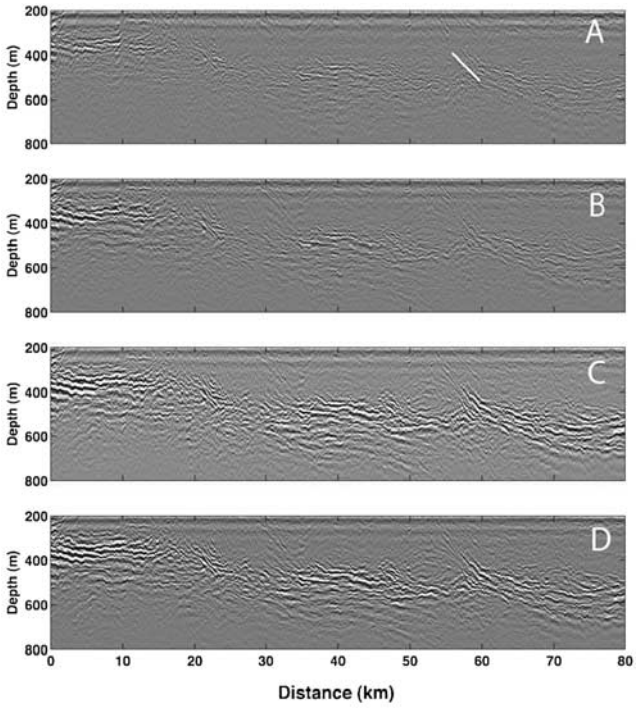

Figure 2. (a) Seismic image produced with sound speed model assuming 1500 m/s. (b) Seismic image produced with sound speed model from Levitus database. (c) Seismic image produced with sound speed model from 17 XBTs. (d) Seismic image produced with handpicked speeds every 200 CMPs. The white line in Figure 2a indicates the location a visible section of the mentioned M2 tidal beam (see Holbrook et al., submitted manuscript, 2009b).

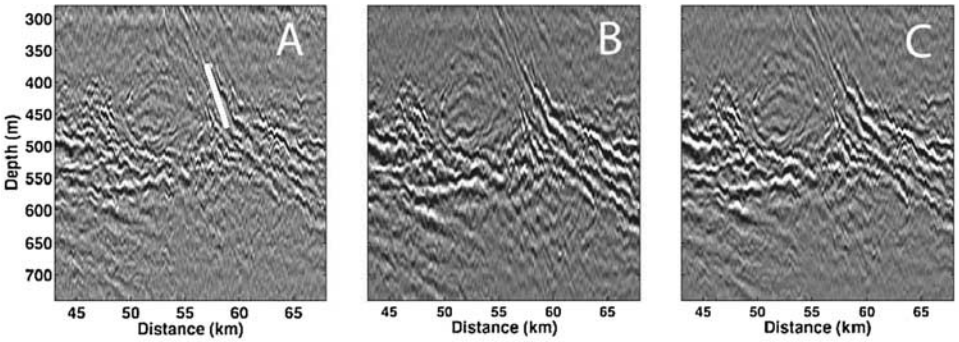

Figure 3. Enlarged sections of the (a) the Levitus-derived seismic image, (b) 17 XBT-derived seismic image, and (c) the handpick-derived image. The white line in Figure 3a indicates the location a visible section of the mentioned M2 tidal beam (see Holbrook et al., submitted manuscript, 2009b).

[18] When processing seismic data for ocean imaging the sound-speed model ultimately defines the clarity of the final image. Without an accurate sound-speed model, quantitative interpretation of seismic images will be inaccurate or even impossible. Simplistic models such as an assumed constant sound speed should be avoided. Except in fortuitous situations, sound-speed models obtained from archived databases are also inadequate to produce clear images. Knowledge of local sound speeds is critical, either from coincident, simultaneous XBTs or user-guided sound speed picking (or both). For data sets that have coincident XBT data, an optimal processing flow would consist of construction of an initial sound-speed model from the XBTs followed by adjustment and interpolation by user-guided model selection.

[19] **Acknowledgments.** This work was supported by Office of Naval Research grant N00014-04-1-0585 and by NSF's Ocean Drilling Program (grant OCE-0221366) and Physical Oceanography Program (grants OCE-0337289, OCE-0452744, and OCE-0648620). We thank the officers and crew of the R/V *Ewing*, and S. Pearse, P. Páramo, P. Nandi, H. Brown, and J. Nealon for data acquisition assistance and initial processing. Data were processed using Paradigm's Focus package, Matlab and Generic Mapping Tools. The authors thank D. Eakin and T. Blacic for valuable discussions.

References

Biescas, B., et al. (2008), Imagine meddy finestructure using multichannel seismic reflection data, *Geophys. Res. Lett.*, *35*, L11609, doi:10.1029/2008GL033971.

Holbrook, W. S., and I. Fer (2005), Ocean internal wave spectra inferred from seismic reflection transects, *Geophys. Res. Lett.*, *32*, L15604, doi:10.1029/2005GL023733.

Holbrook, W. S., et al. (2003), Thermohaline fine structure in an oceanographic front from seismic reflection profiling, *Science*, *301*, 821–824, doi:10.1126/science.1085116.

Klymak, J. M., and J. N. Moum (2007b), Oceanic isopycnal slope spectra. Part II: Turbulence, *J. Phys. Oceanogr.*, *37*, 1232–1245, doi:10.1175/JPO3074.1.

Krahmann, P., et al. (2008), Mid-depth internal wave energy off the Iberian Peninsula estimated from seismic reflection data, *J. Geophys. Res.*, *113*, C12016, doi:10.1029/2007JC004678.

Levitus, S., R. Gelfeld, T. Boyer, and D. Johnson (1994), Results of the NODC and IOC Oceanographic Data Archaeology and Rescue Projects, *Key Oceanogr. Rec. Doc. 19*, Natl. Oceanogr. Data Cent., Washington, D. C.

Mackenzie, K. (1981), Nine-term equation for sound speed in the oceans, *J. Acoust. Soc. Am.*, *70*(3), 807–812, doi:10.1121/1.386920.

Nakamura, Y., et al. (2006), Simultaneous seismic reflection and physical oceanographic observations of oceanic fine structure in the Kuroshio extension front, *Geophys. Res. Lett.*, *33*, L23605, doi:10.1029/2006GL027437.

Nandi, P., et al. (2004), Seismic reflection imaging of water mass boundaries in the Norwegian Sea, *Geophys. Res. Lett.*, *31*, L23311, doi:10.1029/2004GL021325.

Páramo, P., and W. S. Holbrook (2005), Temperature contrasts in the water column calculated through AVO analysis of seismic reflection data, *Geophys. Res. Lett.*, *32*, L24611, doi:10.1029/2005GL024533.

Sheriff, R. E., and L. P. Geldart (1995), *Exploration Seismology*, Cambridge Univ. Press, Cambridge, U. K.

Skagseth, Ø. (2004), Monthly to annual variability of the Norwegian Atlantic slope current: Connection between the northern North Atlantic and the Norwegian Sea, *Deep Sea Res., Part I*, *51*, 349–366, doi:10.1016/j.dsr.2003.10.014.

Swift, J. H. (1986), The Arctic waters, in *The Nordic Seas*, edited by B. G. Hurdle, pp. 129–153, Springer, New York.

Tsuji, T., et al. (2005), Two-dimensional mapping of fine structures in the Kuroshio Current using seismic reflection data, *Geophys. Res. Lett.*, *32*, L14609, doi:10.1029/2005GL023095.

Wood, W., et al. (2008), Full waveform inversion of reflection seismic data for ocean temperature profiles, *Geophys. Res. Lett.*, *35*, L04608, doi:10.1029/2007GL032359.

Yilmaz, O., and S. M. Doherty (1987a), *Seismic Data Processing*, vol. 1, Soc. of Explor. Geophys., Tulsa, Okla.

Yilmaz, O., and S. M. Doherty (1987b), *Seismic Data Processing*, vol. 2, Soc. of Explor. Geophys., Tulsa, Okla.

W. F. J. Fortin and W. S. Holbrook, Department of Geology and Geophysics, University of Wyoming, 1000 East University Avenue, Laramie, WY 82071, USA. (willfortin@gmail.com)